Application of Fragment Screening by X-ray Crystallography to the Discovery of Aminopyridines as Inhibitors of β-Secretase[§]

Miles Congreve,*,[†] David Aharony,[‡] Jeffrey Albert,[‡] Owen Callaghan,[†] James Campbell,[‡] Robin A. E. Carr,[†] Gianni Chessari,[†] Suzanna Cowan,[†] Philip D. Edwards,[‡] Martyn Frederickson,[†] Rachel McMenamin,[†] Christopher W. Murray,[†] Sahil Patel,[†] and Nicola Wallis[†]

Astex Therapeutics Ltd., 436 Cambridge Science Park, Milton Road, Cambridge CB4 0QA, United Kingdom, and Departments of Chemistry and Neuroscience, AstraZeneca Research and Development, 1800 Concord Pike, Wilmington, Delaware 19707

Received October 13, 2006

Fragment-based lead discovery has been successfully applied to the aspartyl protease enzyme β-secretase (BACE-1). Fragment hits that contained an aminopyridine motif binding to the two catalytic aspartic acid residues in the active site of the enzyme were the chemical starting points. Structure-based design approaches have led to identification of low micromolar lead compounds that retain these interactions and additionally occupy adjacent hydrophobic pockets of the active site. These leads form two subseries, for which compounds **4** (IC_{50} = 25 μM) and **6c** (IC_{50} = 24 μM) are representative. In the latter series, further optimization has led to **8a** (IC_{50} = 690 nM).

Introduction

Alzheimer's disease (AD[a]) is a neurodegenerative disorder associated with accumulation of amyloid plaques and neurofibrillary tangles in the brain.[1] The major components of these plaques are β-amyloid peptides (Aβs), which are produced from amyloid precursor protein (APP) by the activity of β- and γ-secretases. β-Secretase cleaves APP to reveal the N-terminus of the Aβ peptides.[2] The β-secretase activity has been identified as the aspartyl protease beta-site APP cleaving enzyme (BACE-1), and this enzyme is a potential therapeutic target for treatment of AD.[3−7]

BACE-1 inhibitors have recently been reviewed.[8,9] Most work has concentrated on the design of peptidomimetic inhibitors which usually employ a secondary alcohol as a transition state mimetic to displace the water molecule that sits between the two catalytic aspartic acids of the enzyme.[10−19] A potential problem with peptidomimetics is that they tend to be relatively large and possess multiple hydrogen bond donors which may make them less attractive leads for a project which requires penetration across the blood−brain barrier and oral bioavailability.[20,21] There has also been some work on the design of less peptidic[22,23] or nonpeptidic inhibitors[24−26] of BACE-1 although in the latter case, there have been no crystal structures to support the binding modes proposed or to develop SAR. There is therefore a great deal of interest in the identification of nonpeptidic inhibitors of BACE-1 and in the experimental determination of their associated binding modes.

We have previously reported the X-ray crystal structure of BACE-1 in its apo form and complexed with a peptidomimetic inhibitor.[27] A representation of the inhibitor bound to the active site of BACE-1 is given in Figure 1. The molecule forms a

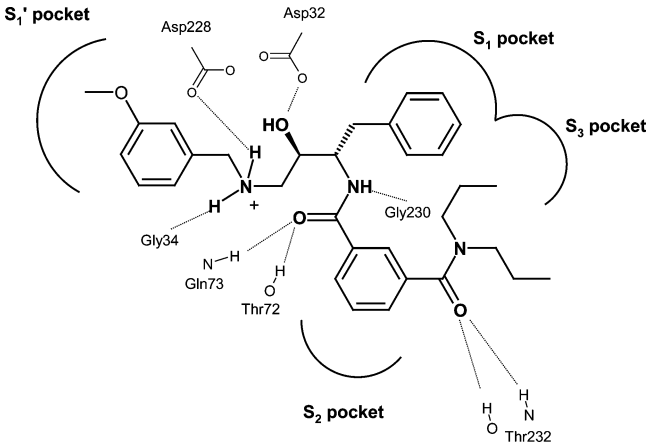

Figure 1. A representation of binding mode of a hydroxyethylamine inhibitor bound to the active site of BACE-1. Hydrogen bonds to residues are shown as broken lines.

number of key hydrogen bonds with the catalytic aspartate residues, but the recognition in this region is somewhat different to that seen with many other secondary alcohol-containing peptide-based inhibitors.[28,29] This highlights the importance of these hydrogen bonds but underlines that there are different ways that inhibitors can favorably make interactions with the catalytic residues. The molecule also forms two hydrogen bonds with the flap region of the active site, and the flap conformation is essentially identical to the flap-closed conformation adopted in published structures of the potent peptide-based inhibitor OM99-2.[28] Additionally, the flap residue, Tyr71, forms two edge-face stacking interactions with the phenyl rings of the inhibitor which lie within the S_1 and S_2' pockets. The inhibitor adopts a 'collapsed' conformation in which one of the *N*-propyl groups packs against a phenyl ring (see Figure 1). These groups then form a continuous surface that fills the large hydrophobic S_1 and S_3 pocket(s) of the enzyme, and this appears to be another key region for BACE-1 inhibition. This knowledge of how substrate-like inhibitors bind to the enzyme was an insightful guide for the structure-based optimization of nonpeptidic fragment hits described below.

In the preceding article in this journal we outlined how fragment screening using protein−ligand X-ray crystallography

§ Coordinates for the β-secretase complexes with compounds **3**, **4**, **6a**, **6b**, **7**, and **8b** have been deposited in the Protein Data Bank under accession codes 2OHP, 2OHQ, 2OHR, 2OHS, 2OHT and 2OHU, together with the corresponding structure factor files.

* To whom correspondence should be addressed. Phone: +44 (0)1223 226270; Fax +44 (0)1223 226201; E-mail: m.congreve@astex-therapeutics.com.

† Astex Therapeutics Ltd.

‡ AstraZeneca Research and Development.

[a] Abbreviations. AD, Alzheimer's disease; APP, amyloid precursor protein; BACE-1, beta-site APP cleaving enzyme; LE, ligand efficiency.

10.1021/jm061197u CCC: $37.00
Published on Web 02/22/2007

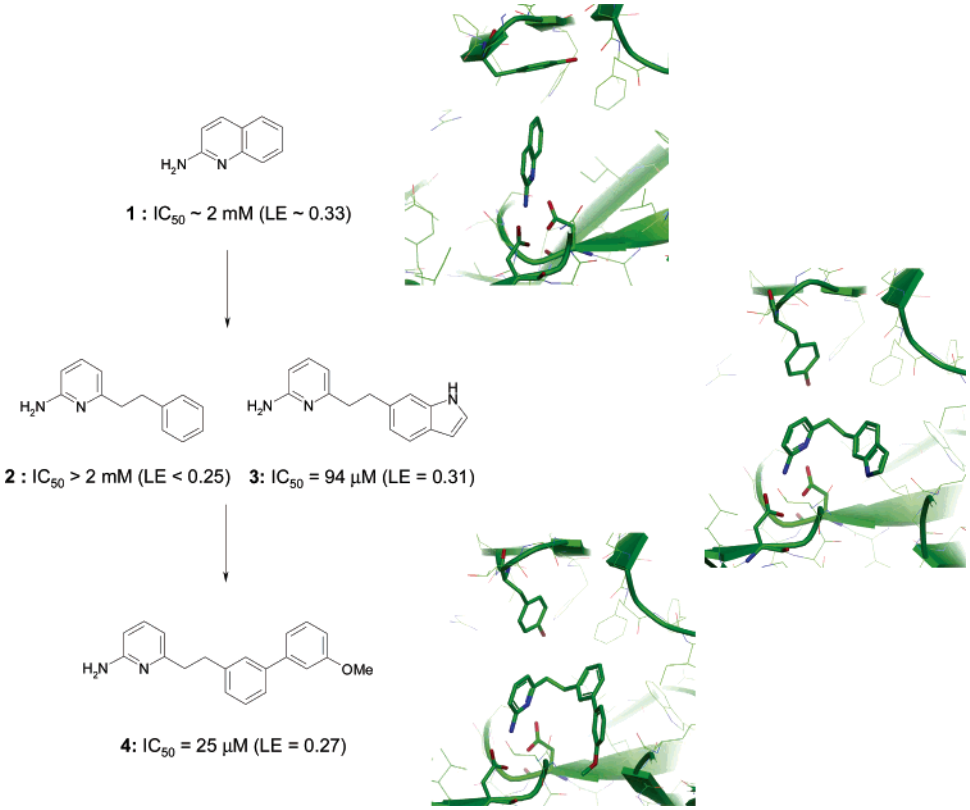

Figure 2. The binding mode of 6-substituted 2-aminopyridine inhibitors in the active site of BACE-1. On the left, a schematic representation of the inhibitors is provided together with available IC_{50} data. The experimental binding mode appears on the right-hand side with the protein backbone represented as a cartoon and the protein atoms in thin stick. The ligand and the residues Asp32, Tyr71 and Asp228 are represented in thick stick. In this orientation the flap is toward the top of the picture and the S_1 and S_3 pockets are on the right.

had identified a series of ligands that bound to the catalytic aspartic acid residues in the active site of BACE-1 through an amidine or aminopyridine motif. This type of charged bidentate interaction has not previously been described between inhibitor molecules and aspartyl protease enzymes. Using this finding as a starting point, virtual screening of related molecules identified a number of attractive fragments for structure-based optimization. The syntheses of aminopyridine analogues, the biological activity, and the protein−ligand interactions made by the more potent inhibitors are outlined in this article.

Results and Discussion

6-Substituted 2-Aminopyridine Inhibitors. The preceding article describes discovery of 2-aminoquinoline **1** as one ligand that binds to the active site of BACE-1. The principle interactions are between the charged aminopyridine motif and the two catalytic aspartates of the enzyme. The region adjacent to this ligand is the S_1 pocket, which is a highly hydrophobic area of the active site, and was attractive to target. 2-Aminoquinoline **1** had unsuitable vectors to easily target this region of the active site. Instead, a consideration of the binding mode of fragment **1**, in which the fused phenyl ring is adjacent to the S_1 pocket, led us to design 6-substituted phenylethyl-2-aminopyridine **2** (Figure 2). In this design the phenyl group was predicted to make good hydrophobic contact with the S_1 region. A comparison of the crystal structures of **1** and **2** indicated that the aminopyridine moiety retained the bidentate binding to the catalytic aspartic acid residues (Asp32 and Asp228) and that, as expected, the phenyl substituent occupied the S_1 pocket. The structure of **2** was of low resolution,[30] but this new derivative still represented a more useful starting point for further compound design than 2-aminoquinoline itself.

The next target selected was the indole-substituted aminopyridine **3** (Figure 2). This compound was designed to better occupy the S_1 pocket by incorporating a larger bicyclic ring system in the hydrophobic pocket, compared with the phenyl-substituted precursor **2**. The crystal structure of **3** is illustrated in Figure 2 and clearly indicates how the indole occupies the S_1 region. In addition, a new interaction was observed between the indole NH and the backbone carbonyl of Gly230 on the edge of the S_3 pocket. The S_1 and S_3 regions are contiguous in BACE-1, and the S_3 pocket is again rather hydrophobic in nature. Testing of this analogue in the enzyme assay gave an $IC_{50} = 94\ \mu M$, indicating that the indole moiety was indeed forming favorable contacts in the S_1-S_3 region of the site and that this was a useful area to target in the next iteration of design.

A consideration of the van der Waals contacts between **3** and the S_1-S_3 hydrophobic pocket suggested that larger hydrophobic groups should be tolerated in this region. A small number of derivatives were designed and synthesized, and one of the more promising analogues made was **4** in which a 3-methoxy-biaryl group replaced the indole substituent. Figure 2 shows how this group makes good contact with the active site. Notably there is a change in conformation of the flap region of the enzyme, so that Tyr71 moves and rotates above the aminopyridine ring, better accommodating the ligand. The twist out of plane of the second aromatic ring of the biaryl, relative to the indole of **3**, helps improve hydrophobic contact with the pocket. Additionally, the methoxy group pendent to the biaryl moiety complements a small, more polar area by displacing a water molecule at the bottom of the S_3 pocket and forms an H-bonding interaction with the backbone NH of Gly13. The potency of **4** is improved, in comparison to **3**, to $IC_{50} = 25\ \mu M$, and this compound represented a good lead molecule for further design

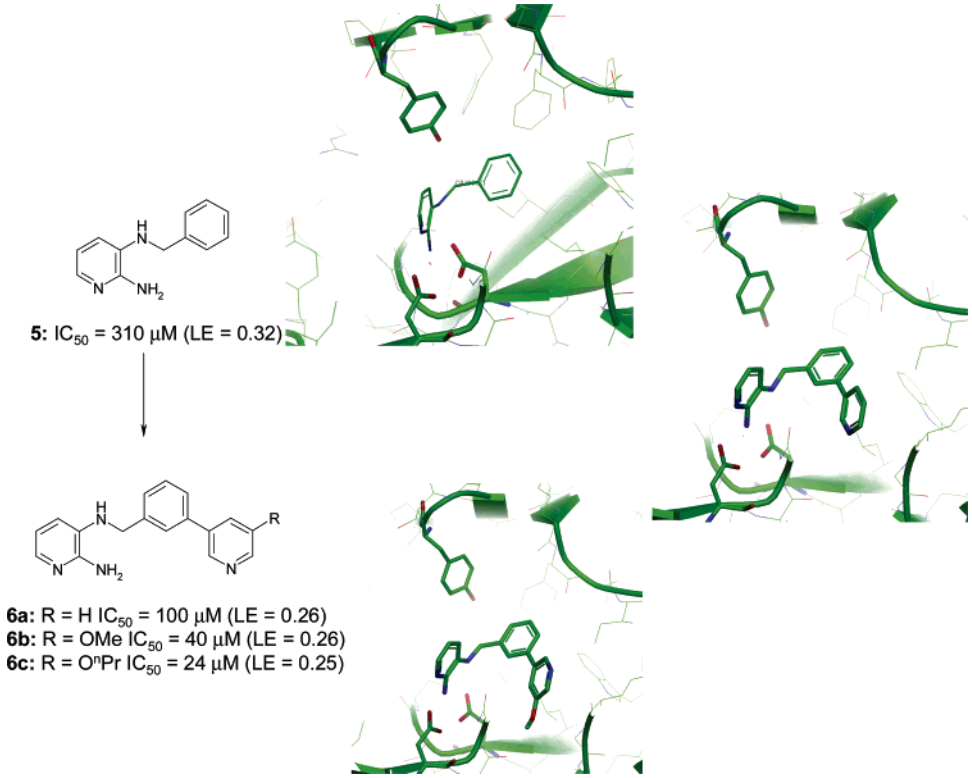

Figure 3. The binding mode of 3-substituted 2-aminopyridine inhibitors in the active site of BACE-1. On the left, a schematic representation of the inhibitors is provided together with available IC_{50} data. The experimental binding mode appears on the right-hand side with the protein backbone represented as a cartoon and the protein atoms in thin stick. The ligand and the residues Asp32, Tyr71 and Asp228 are represented in thick stick. In this orientation the flap is toward the top of the picture and the S_1 and S_3 pockets are on the right.

and elaboration. In particular, the biaryl motif was suitable for further substitution and modification, and there were additional vectors on the aminopyridine ring itself suitable for exploration of the prime side of the active site.

3-Substituted 2-Aminopyridine Inhibitors. Virtual screening of aminopyridine derivatives from commercial sources and from the Astex compound collection identified 2,3-diaminopyridine **5** as a hit *in silico*. The subsequent soaking of this molecule into crystals of the enzyme indicated that binding did indeed take place (Figure 3). This is described in some detail in the sister publication. The aminopyridine again forms a charged bidentate interaction with the catalytic aspartates of the active site; however, in this case the molecule has changed orientation relative to the fragment hit **1**. This new binding mode allows an additional interaction to form between the 3-amino group which donates its hydrogen atom to Asp32. This switch in orientation of the aminopyridine ring allows the *N*-benzyl group of the compound to occupy the S_1 pocket, again demonstrating the enzyme's preference for hydrophobic binding to this pocket. This analogue **5** gave an $IC_{50} = 310\ \mu M$ in the enzyme assay, which we considered to be promising potency for such a small fragment against this very challenging target.

Using the insight we had gained from the work described above in the 6-substituted 2-aminopyridine series, a small number of biaryl substituted 2,3-diaminopyridine targets were designed to better occupy the S_1-S_3 hydrophobic pocket. Introduction of a 3-substituted 3-pyridyl group was found to be particularly useful because these analogues gave excellent quality protein−ligand crystal structures (Figure 3), probably due to the 3-pyridyl phenyl group forming favorable contacts with the pocket and because the pyridyl group improved aqueous solubility of these ligands. Interestingly, the pyridyl nitrogen forms an H-bond with a water molecule at the bottom of the S_3 pocket in compound **6a**. In the complex of **4** described earlier (Figure 2) the methoxy group had displaced this water molecule. The potency of **6a** was $IC_{50} = 100\ \mu M$, a reasonable improvement over the parent compound **5**. Taken together these data indicated that there were profitable interactions to be made by occupying the S_3 pocket and by targeting the more polar region at the bottom of this pocket.

The next analogues identified contained either a methoxy group (**6b**) or a propyloxy group (**6c**) in addition to the pyridyl nitrogen atom at the meta-positions of the ring system and were designed in order to understand whether the best interactions involved displacement of the water molecule in this region, or binding to it. Figure 3 shows the complex of **6c**. For this ligand, as well as in **6b**, the oxygen atom of the ligand displaces the water molecule that had been targeted, and the alkyl group is positioned within the narrow opening at the bottom of the S_3 pocket. The methoxy derivative **6b** had an $IC_{50} = 40\ \mu M$ and the propyloxy compound **6c** an $IC_{50} = 24\ \mu M$, indicating that the addition of the propyloxy substituent increased affinity compared with **6a** ($IC_{50} = 100\ \mu M$). At this point we considered analogue **6c** to be a good quality lead molecule, particularly as analogues in the 2,3-diaminopyridine series benefited from a short and convenient synthesis (described later). This series was therefore prioritized over the 6-substituted 2-aminopyridines outlined earlier for the next round of compound design.

Identification of a Sub-micromolar Inhibitor. Having successfully optimized the 3-substituted 2-aminopyridine series to low micromolar potency, higher molecular weight inhibitors were designed, first to better fill the S_3 pocket, and second to target substituents beneath the 'flap' region of the active site. The objective of this work was to establish if it was possible to identify nonpeptidic inhibitors with sub-micromolar affinity for the BACE-1 enzyme. It was rationalized that modification of the substituted pyridyl ring to a bicyclic heterocycle might better occupy the S_3 pocket, and 6-indolyl was one of the modifications

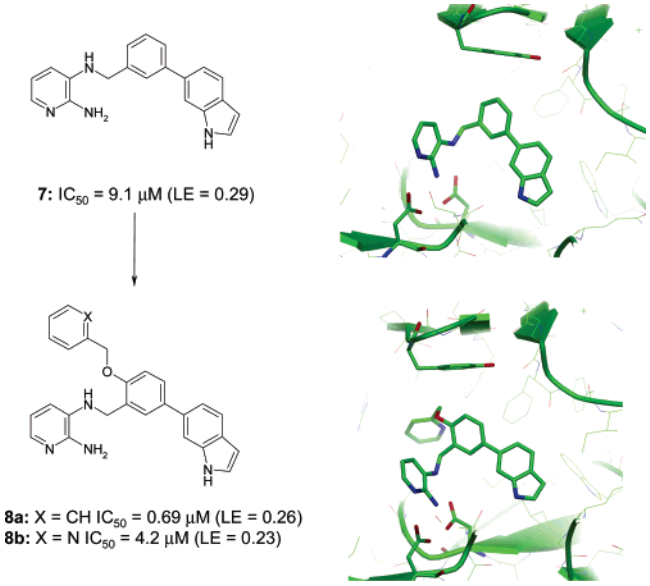

Figure 4. The optimization of 3-substituted 2-aminopyridine ligands in the active site of BACE-1. On the left, a schematic representation of the inhibitors is provided together with available IC_{50} data. The experimental binding mode appears on the right-hand side with the protein backbone represented as a cartoon and the protein atoms in thin stick. The ligand and the residues Asp32, Tyr71 and Asp228 are represented in thick stick. In this orientation the flap is toward the top of the picture and the S_1 and S_3 pockets are on the right.

chosen to probe this question. Figure 4 illustrates the binding mode of this derivative **7** to BACE-1. Compared with the biaryl-containing inhibitors **6a**−**c**, the phenyl ring of this ligand sits higher in the S_1 pocket, and there is a small rotation of the 2,3-diaminopyridine moiety, but without causing any disruption of its interactions with the two catalytic aspartates. The indolyl group sits in S_3 as expected and forms a new interaction between the NH of the heterocycle and the backbone carbonyl of Gly230. This compound had an affinity of $IC_{50} = 9.1\ \mu M$.[31] The position of the phenyl ring suggested that the ortho-position, adjacent to the methylene linking the ring to the 2,3-diaminopyridine, might be a useful vector to explore substitution under the 'flap' toward the S_2' region. It has been observed that piperidine-based inhibitors of renin are capable of binding groups in a similar region, whereupon a significant protein conformational change occurs, opening a large hydrophobic pocket.[32−34] To this end, two compounds were synthesized in which a benzyloxy (**8a**) or a 2-pyridinylmethyloxy group (**8b**) was added (Figure 4). These compounds had affinities of $IC_{50} = 0.69\ \mu M$ (**8a**) and 4.2 μM (**8b**), respectively. The benzyloxy compound was not sufficiently soluble to afford a high quality crystal structure; however, the pyridyl-containing **8b** did give a useful complex. The new substituent does not effect a significant protein conformational change and occupies the S_2' pocket of the enzyme as expected, making hydrophobic contact and forming a hydrogen bond between the side chain NH of Trp76 and the pyridyl nitrogen atom. The 2,3-diaminopyridine and phenylindolyl groups bind in an identical fashion to compound **7**. It is likely that the sub-micromolar inhibitor **8a** adopts a similar overall binding mode.

Ligand Efficiency. In the previous publication in this issue the ligand efficiencies (LE) of the aminopyridine-containing fragments discovered using high throughput crystallography were described. Aminoquinoline **1** has an estimated LE = 0.33 according to Hopkins's formula:[35]

$$LE = -\Delta G/HAC \approx -RT \ln(IC_{50})/HAC$$

This compares favorably with published peptide-based inhibitors[28,29] that have low LE (<0.2). A ligand having a value >0.3 is consistent with identifying a compound with a molecular weight <500 Da and potency in the 10 nM range. The LE values for the compounds identified during the work described above have been added to Figures 2−4. It can be seen that the most potent compounds have LE generally in the range 0.25−0.29, just below the target value of 0.3. These values are significantly superior to known peptide-based inhibitors and would suggest that lead optimization could result in identification of potent inhibitors with an acceptable molecular weight range.

Conclusions

Two series of micromolar potency nonpeptidic inhibitors of BACE-1 have been successfully identified and crystallized in the enzyme active site. These two novel compound classes include a binding motif not previously observed in aspartic protease inhibitors.[36] Further studies in which use of this pharmacophore has allowed identification of nanomolar inhibitors will be the subject of future publications.

Experimental Section

Crystallography. Recombinant human β-secretase 1 (BACE-1), residues 14−453, was produced in bacteria as inclusion bodies and refolded using a method described previously.[27] Crystals of apo BACE-1 suitable for ligand soaking were obtained by a procedure described by Patel et al.[27] In brief, BACE-1 was buffer-exchanged into 20 mM Tris (pH 8.2), 150 mM NaCl, and 1 mM DTT and concentrated to 8 mg/mL. DMSO (3% v/v) was added to the protein prior to crystallization. Apo BACE-1 crystals were grown using the hanging drop vapor diffusion method at 20 °C. Protein was mixed with an equal volume of mother liquor containing 20−22.5% (w/v) PEG 5000 monomethylethyl (MME), 200 mM sodium citrate (pH 6.6), and 200 mM ammonium iodide. Crystals were cryoprotected for data collection by brief immersion in 30% PEG 5000 MME, 100 mM sodium citrate (pH 6.6), 200 mM ammonium iodide, and 20% (v/v) glycerol. For inhibitor soaking, 0.5−0.1 M DMSO stock solutions were made. A tenfold dilution of the compound stock solution in a stabilization solution (33% (w/v) PEG 5000 monomethylethyl (MME), 110 mM sodium citrate (pH 6.6), and 220 mM ammonium iodide) was made. Crystals were added to the soaking solution for up to 6 h prior to flash freezing and data collection. Data were collected at a number of synchrotron beam lines at the European Synchrotron Radiation Facility, Grenoble, France. All data sets were processed with MOSFLM[37] and scaled using SCALA.[38] Structure solution and initial refinement of the protein−ligand complexes were carried out by our automated scripts using a modified apo BACE-1 structure (PDB id code 1w50) as a starting model. Bound ligands were automatically identified and fitted into $F_o - F_c$ electron density using AutoSolve[39] and further refined using automated scripts followed by rounds of rebuilding in AstexViewer2[40] and refinement using Refmac.[41] Data collection and refinement statistics for crystal structures are presented in Table 1.

BACE-1 Assays. Activity of BACE-1 was measured using the peptide R-E(EDANS)-E-V-N-L-*D-A-E-F-K(DABCYL)-R-OH from Bachem. Assays were carried out in 50 mM sodium acetate, pH 5, 10% DMSO, in 96-well black, flat bottomed Cliniplates in a final assay volume of 100 μL. Compounds were preincubated with in-house produced BACE-1, and the reaction was initiated by adding 10 μM peptide substrate. The reaction rate was monitored at room temperature on a Fluoroskan Ascent platereader with excitation and emission wavelengths of 355 and 530 nm, respectively. Initial reaction rates were measured, and IC_{50}s were calculated from replicate curves using GraphPad Prizm software.

Table 1. Crystallographic Data Collection and Refinement Statistics[a]

	3	4	6a	6b	7	8b
			Data Collection			
X-ray source	ESRF ID14.1, $\lambda = 0.934$ Å	ESRF ID14.3, $\lambda = 0.931$ Å	ESRF ID14.3, $\lambda = 0.931$ Å	ESRF ID14.3, $\lambda = 0.931$ Å	ESRF ID14.3, $\lambda = 0.931$ Å	in house, $\lambda = 1.54$ Å
resolution (Å)	2.2	2.1	2.2	2.5	2.3	2.4
no. unique reflections	25567	31079	24903	18681	22857	21939
completeness (%)[b]	99.8(100)	99.0(96.0)	98.7(99.4)	95.8(87.3)	99.4(99.4)	98.8(98.0)
average multiplicity	2.6	2.5	2.5	2.3	2.5	2.6
R_{merge}[b]	9.1(36.1)	6.9(31.0)	10.5(39.6)	11.8(43.0)	10.5(37.3)	8.1(36.6)
			Refinement			
R_{free}	28.1	27.6	21.4	25.1	26.9	24.8
R_{cryst}	23.2	21.8	17.0	18.2	21.2	19.5
rmsd bond lengths (Å)	0.013	0.013	0.013	0.013	0.013	0.013
rmsd bond angles (deg)	1.4	1.4	1.4	1.5	1.4	1.4
average *B*-factor protein (Å^2)	44.7	42.8	31.6	30.8	42.4	44.2
average *B*-factor ligand (Å^2)	55.3	54.6	26.5	29.6	47.0	49.0
average *B*-factor solvent (Å^2)	37.4	46.1	37.6	32.1	36.7	40.3

[a] $R_{merge} = \Sigma_h\Sigma_i|I(h,i) - (h)|\ \Sigma hSi\ (h)$; $I(h,i)$ is the scaled intensity of the ith observation of reflection h and (h) is the mean value. Summation is over all measurements. $R_{cryst} = \Sigma_{hkl,work}||F_{obs}| - k|F_{calc}||/\Sigma_{hkl}|F_{obs}|$, where F_{obs} and F_{calc} are the observed and calculated structure factors, k is a weighting factor and work denotes the working set of 95% of the reflections used in the refinement. $R_{free} = \Sigma_{hkl,test}|F_{obs}| - k|F_{calc}||/\Sigma_{hkl}|F_{obs}|$, where F_{obs} and F_{calc} are the observed and calculated structure factors, k is a weighting factor and test denotes the test set of 5% of the reflections used in cross validation of the refinement. λ refers to wavelength, rmsd to root-mean-square deviations. [b] Numbers in parentheses indicate the highest shell values.

Compounds that fluoresced under the conditions described above were assayed in an alternative assay. BACE-1 activity was measured using a FRET-based substrate supplied by PanVera (kit P2985). Assays were carried out in 50 mM sodium acetate, pH 4.5 (provided with kit), 5% DMSO in 96-well black, flat-bottomed 1/2 area Costar plates in a final assay volume of 50 μL. Compounds were preincubated as above for 5 min with in-house-produced BACE-1, and the reaction was initiated by adding 0.25 μM peptide substrate. The reaction rate was monitored at room temperature on a SpectraMax Gemini XS platereader (Molecular Devices) with excitation and emission wavelengths of 545 and 595 nm, respectively. Initial reaction rates were measured, and IC_{50}s were calculated as described above.

Modeling. Docking experiments were used to predict the binding mode of designed aminopyridines and to select compounds for synthesis. The aminoquinoline and aminoisoquinoline BACE-1 structures described in the previous paper were selected to dock the ligands. For each structure, a number of binding sites were constructed. Each of them contained the catalytic region (Asp32 and Asp228) with both Asp residues in the ionized state, the flap residues potentially involved in the binding of the ligands (Val69, Pro70, Tyr71, Thr72, and Trp76), and finally one of the following combinations of adjacent pockets: S_1, S_1 plus S_3, S_2' plus S_1 and a large binding site constituted by S_1, S_1', S_2', and S_3. All dockings were run on a Linux cluster using Goldscore scoring functions within the Astex web-based docking facilities.[42] Methods and settings have been previously described by Verdonk et al.[43]

Chemistry. Reagents and solvents were obtained from commercial suppliers and used without further purification. Thin layer chromatography (TLC) analytical separations were conducted with E. Merck silica gel F-254 plates of 0.25 mm thickness and were visualized with UV light (254 nM) or I_2. Flash chromatography was performed using E. Merck silica gel. ^{1}H nuclear magnetic resonance (NMR) spectra were recorded in the deuterated solvents specified on a Bruker Avance 400 spectrometer operating at 400 MHz. Chemical shifts are reported in parts per million (δ) from the tetramethylsilane resonance in the indicated solvent (TMS: 0.0 ppm). Data are reported as follows: chemical shift, multiplicity (br = broad, s = singlet, d = doublet, t = triplet, m = multiplet), coupling constants (Hz), integration. Compound purity and mass spectra were determined by a Waters Fractionlynx/Micromass ZQ LC/MS platform using the positive electrospray ionization technique (+ES) using a mobile phase of acetonitrile/water with 0.1% formic acid. Compound **5**, N^3-benzyl-pyridine-2,3-diamine was prepared as per Khanna et al.[44]

2-(6-Methylpyridin-2-yl)isoindole-1,3-dione (10a). A mixture of 2-amino-6-methylpyridine **9** (21.6 g, 0.2 mol) and phthalic anhydride (29.6 g, 0.2 mol) were stirred and held at 190 °C for 1 h and then cooled to room temperature to afford **10a** as a pale yellow solid (45.5 g, 95%). ^{1}H NMR (400 MHz, DMSO-d_6): δ 2.52 (s, 3H), 7.37 (d, $J = 7$, 1H), 7.40 (d, $J = 7$, 1H), 7.90−7.95 (m, 3H), 7.97−8.03 (m, 2H). MS (+ES): *m/e* 239 (MH^+).

Scheme 1. Synthesis of 6-Substituted 2-Aminopyridine Inhibitors[a]

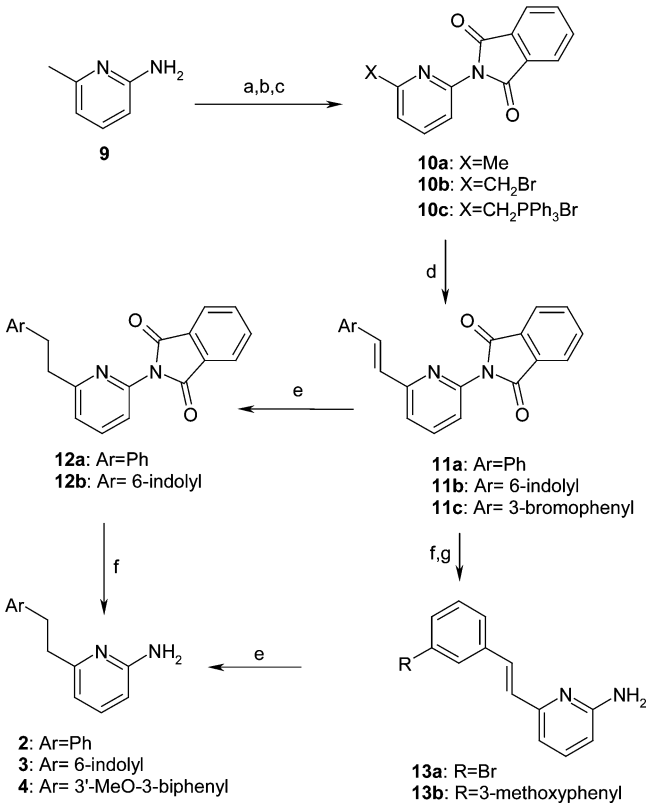

[a] Reagents: (a) Phthalic anhydride, 190 °C; (b) NBS, AIBN, C_6H_6, reflux; (c) PPh_3, MeCN, reflux; (d) ArCHO, KO^{t}Bu, THF, reflux; (e) H_2, 10% Pd on carbon, MeOH; (f) N_2H_4 hydrate, EtOH, reflux; (g) 3-MeO-PhB$(OH)_2$, K_2CO_3, Pd$(P^tBu_3)_2$, PhMe, H_2O, EtOH, MeOH, microwave irradiation, 135 °C.

[6-(1,3-Dioxo-1,3-dihydroisoindol-2-yl)pyridin-2-ylmethyl]-triphenylphosphonium Bromide (10c). A mixture of the 2-(6-methylpyridin-2-yl)isoindole-1,3-dione **10a** (23.8 g, 0.1 mol), *N*-bromosuccinimide (19.0 g, 0.11 mol), and AIBN (1.2 g) in anhydrous benzene (400 mL) was stirred and held at reflux for 5

Scheme 2. Synthesis of 3-Substituted 2-Aminopyridine Inhibitors[a]

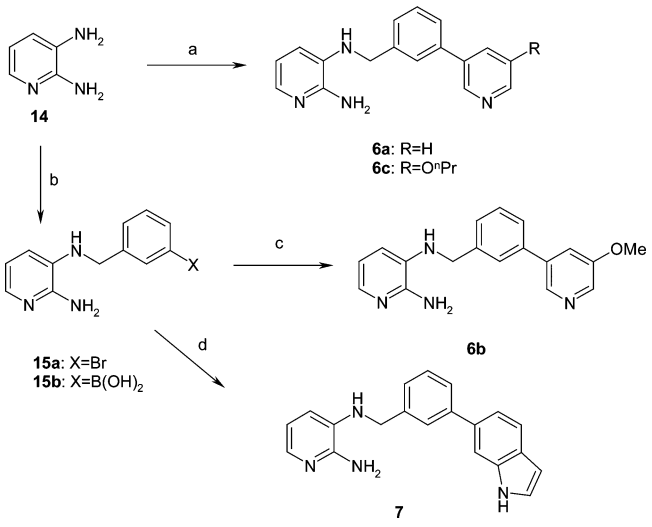

[a] Reagents: (a) Aryl aldehyde, AcOH, $NaBH(OAc)_3$, CH_2Cl_2; (b) aryl aldehyde, Et_3N, $NaBH(OAc)_3$, 4 Å sieves, CH_2Cl_2; (c) **15a**, 5-methoxypyridyl-3-boronic acid, K_2CO_3, $Pd(P^tBu_3)_2$, EtOH, MeOH, toluene, water, 135 °C, microwave; (d) **15b**, 6-bromoindole, K_3PO_4,$Pd(PPh_3)_4$, DMF, 100 °C.

Scheme 3. Synthesis of 3-Substituted 2-Aminopyridine Inhibitors[a]

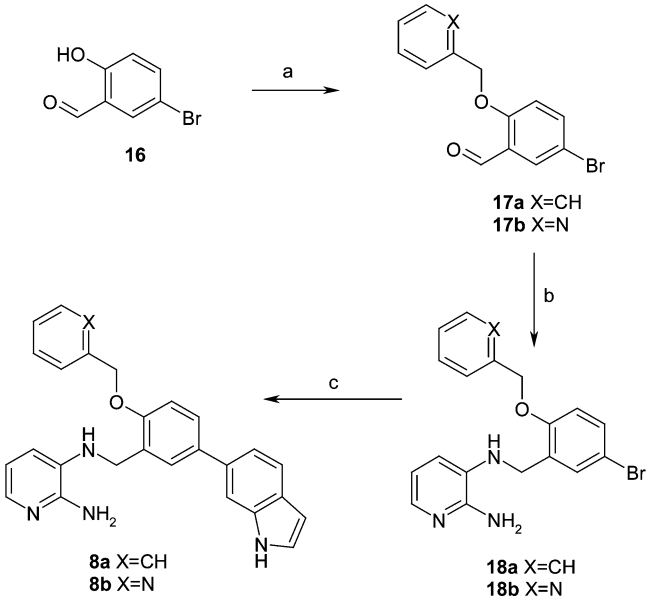

[a] Reagents: (a) Benzylic halide, K_2CO_3, THF, reflux; (b) 2,3-diaminopyridine, AcOH, $NaBH(OAc)_3$, CH_2Cl_2; (c) indole-6-boronic acid, K_2CO_3, $Pd(P^tBu_3)_2$, PhMe, H_2O, EtOH, MeOH, microwave irradiation, 135 °C.

h. The mixture was cooled to room temperature and then chilled in an ice bath for 10 min with vigorous stirring. The insoluble material was removed by filtration and the solvent removed *in vacuo*. The resulting solid crude benzylic bromide **10b** was dissolved in acetonitrile (400 mL), triphenylphosphine (26.2 g, 0.1 mol) was added, and the mixture was stirred and held at reflux for 16 h. Upon cooling, the solid material was collected by suction filtration, washed with acetonitrile, and sucked dry to afford **10c** as a colorless solid (36.75 g, 63%).^{1}H NMR (400 MHz, DMSO-d_6): δ 5.54 (d, J = 18, 2H), 7.43 (m, 2H), 7.62−7.68 (m, 6H), 7.78−7.85 (m, 9H), 7.95−8.02 (m, 5H). MS (+ES): *m/e* 499 (M^+).

2-[6-((*E*)-Styryl)pyridin-2-yl]isoindole-1,3-dione (11a). Potassium *tert*-butoxide (260 mg, 2.32 mmol) was added to a stirred suspension of **10c** (1.16 g, 2.0 mmol) in anhydrous tetrahydrofuran (30 mL), and the mixture was stirred at room temperature for 15 min. Benzaldehyde (224 mg, 2.11 mmol) was added, and the mixture was stirred and held at reflux for 6 h. Upon cooling to room temperature, the solvent was removed *in vacuo* and the mixture partitioned between dichloromethane and water. The organic layer was separated, the solvent removed *in vacuo*, and the residue subjected to column chromatography on silica. Elution with diethyl ether afforded **11a** as a pale yellow solid (420 mg, 65%). ^{1}H NMR (400 MHz, DMSO-d_6): δ 7.33−7.46 (m, 5H), 7.65−7.76 (m, 4H), 7.95−8.02 (m, 2H), 8.03−8.08 (m, 3H). MS (+ES): *m/e* 327 (MH^+).

Compounds **11b** and **11c** were prepared in a similar fashion to that outlined above for **11a**. For NMR and MS data of these compounds, see Supporting Information.

2-(6-Phenethylpyridin-2-yl)isoindole-1,3-dione (12a). 10% Palladium on carbon (80 mg) was added to **11a** (260 mg, 0.80 mmol) in methanol (10 mL) and ethyl acetate (5 mL), and the mixture was stirred at room temperature under a hydrogen atmosphere for 16 h. The catalyst was removed by filtration, and the solvent was removed *in vacuo* to afford crude **12a** as a colorless oil (250 mg, 96%) which was used without further purification. ^{1}H NMR (400 MHz, DMSO-d_6): δ 3.02 (m, 2H), 3.08 (m, 2H), 7.18 (m, 1H), 7.25 (m, 4H), 7.37 (t, J = 7, 2H), 7.95 (m, 3H), 8.02 (m, 2H). MS (+ES): *m/e* 329 (MH^+).

Compound **12b** was prepared in a similar fashion to that outlined above for **12a**. For NMR and MS data of this compound, see Supporting Information.

6-Phenethylpyridin-2-ylamine (2). Hydrazine hydrate (103 mg, 2.06 mmol) was added to a solution of **12a** (210 mg, 0.64 mmol) in ethanol (8 mL), and the mixture was stirred and held at reflux for 3 h. Upon cooling, the solvent was removed *in vacuo* and the residue partitioned between dichloromethane and water. The organic layer was separated, the solvent removed *in vacuo*, and the residue subjected to column chromatography on silica. Elution with diethyl ether afforded **2** as a pale yellow oil (95 mg, 75%). ^{1}H NMR (400 MHz, DMSO-d_6): δ 2.77 (t, J = 7, 2H), 2.90 (t, J = 7, 2H), 5.82 (br s, 2H), 6.26 (d, J = 8, 1H), 6.34 (d, J = 8, 1H), 7.18 (t, J = 8, 1H), 7.15−7.30 (m, 5H). MS (+ES): *m/e* 199 (MH^+).

Compounds **3** and **13a** were prepared in a similar fashion to that outlined above for **2**. For NMR and MS data of these compounds, see Supporting Information.

6-[2-(3′-Methoxybiphenyl-3-yl)ethyl]pyridin-2-ylamine (4). A mixture of **13a** (110 mg, 0.4 mmol), 3-methoxyphenylboronic acid (92 mg, 0.6 mmol), anhydrous potassium carbonate (276 mg, 2.0 mmol), and bis(tri-*tert*-butylphosphine)palladium(0) (5 mg) in methanol (1 mL), ethanol (1 mL), water (1 mL), and toluene (1 mL) was subjected to microwave irradiation (CEM microwave) at 135 °C for 30 min. The mixture was filtered, the organic solvent evaporated *in vacuo*, and the residue partitioned between dichloromethane and 1 M sodium hydroxide. The organic layer was separated and the solvent removed *in vacuo* to afford crude **13b.** Methanol (15 mL) and 10% palladium on carbon (60 mg) were added, and the mixture was stirred under an atmosphere of hydrogen for 5 h. The catalyst was removed by filtration, the solvent was removed *in vacuo*, and the residue was subjected to column chromatography on silica. Elution with ethyl acetate afforded **4** as a colorless oil (85 mg, 70%). ^{1}H NMR (400 MHz, DMSO-d_6): δ 2.83 (t, 2H, J = 7), 3.00 (t, 2H, J = 7), 3.83 (s, 3H), 5.80 (br s, 2H), 6.27 (d, 1H, J = 8), 6.37 (d, 1H, J = 7), 6.93 (dm, J = 8, 1H), 7.14 (t, J = 1.5, 1H), 7.18−7.30 (m, 3H), 7.33−7.39 (m, 2H), 7.47 (m, 2H). MS (+ES): *m/e* 305 (MH^+).

***N*^{3}-(3-Pyridin-3-ylbenzyl)pyridine-2,3-diamine (6a)**. A mixture of 2,3-diaminopyridine (327 mg, 3.0 mmol), 3-pyridin-3-ylbenzaldehyde (3.0 mmol), and acetic acid (8−10 drops) in dichloromethane (15 mL) was stirred at room temperature for 30 min. Sodium triacetoxyborohydride (1.91 g, 9.0 mmol) was added and the mixture stirred at room temperature overnight. The mixture was washed with an equal volume of 10% aqueous potassium carbonate solution, the organic layer separated, the solvent removed *in vacuo*, and the residue purified by column chromatography on silica. Elution with mixtures of ethyl acetate and methanol afforded the product. ^{1}H NMR (400 MHz, $CDCl_3$): δ 3.65 (br s, 1H), 4.23 (br s, 2H), 4.38 (d, J = 4.8, 2H), 6.79 (dd as t, J = 6.0, 1H), 6.84

(d, $J = 7.5$, 1H), 7.37 (dd, $J = 7.9$, 4.2, 1H), 7.43 (d, $J = 7.3$, 1H), 7.47 (d, $J = 7.6$, 1H), 7.51 (t, $J = 6.5$, 1H), 7.59 (s, 1H), 7.63 (d, $J = 5.0$, 1H), 7.86 (d, $J = 7.8$, 1H), 8.60 (d, $J = 4.8$, 1H), 8.84 (s, 1H). MS (+ES): *m*/*e* 277 (MH^+).

***N*³-(3-Bromobenzyl)pyridine-2,3-diamine (15a)**. To a stirred solution of 2,3-diaminopyridine (5 g, 45.8 mmol) in DCM (200 mL) were added 3-bromobenzaldehyde (5.37 mL, 45.8 mmol), triethylamine (19.2 mL, 137 mmol), and 4 Å molecular sieves followed by sodium triacetoxyborohydride (38.8 g, 183 mmol). The reaction was allowed to stir at RT for 16 h. The reaction was monitored by TLC, and further equivalents of sodium triacetoxyborohydride were added as required. The mixture was filtered and then diluted with DCM, washed with H_2O, and dried over $MgSO_4$ and the solvent removed *in vacuo*. The residue was purified by column chromatography eluting with 5% MeOH in DCM to give the title compound as a pale yellow oil (4.33 g, 34%). ^{1}H NMR (400 MHz, MeOH-d_4): δ 4.40 (s, 2H), 6.62 (dd, $J = 7.8$, 5.5, 1H), 6.73 (dd, $J = 7.6$, 1.2, 1H), 7.24−7.33 (m, 2H), 7.38 (d, $J = 7.6$, 1H), 7.43 (br d, $J = 8.0$, 1H), 7.58 (s,1H). MS (+ES): *m*/*e* 278, 280 (MH^+).

Compound **15b** was prepared in a similar fashion to that outlined above for **15a**, but in this case no aqueous work up procedure was used. For NMR and MS data of this compound, see Supporting Information.

***N*³-[3-(5-Methoxypyridin-3-yl)benzyl]pyridine-2,3-diamine (6b)**. To a degassed solution of *N*³-(3-bromobenzyl)pyridine-2,3-diamine (100 mg, 0.36 mmol) in toluene (1.5 mL) was added bis(tri-*tert*-butylphosphine)palladium(0) (5 mg) followed by 5-methoxypyridyl-3-boronic acid (202 mg, 0.86 mmol) as a solution in ethanol (1.5 mL). Potassium carbonate (299 mg, 2.16 mmol) was then added as a solution in H_2O (2 mL) followed by methanol (2 mL). The reaction was heated to 135 °C for 35 min in a CEM microwave. The mixture was cooled to room temperature and the solvent removed *in vacuo*. The resulting material was partitioned between DCM and H_2O, dried over $MgSO_4$, and evaporated to dryness. Material purified by preparative HPLC to give the title compound as a pale yellow solid (41 mg, 37%). ^{1}H NMR (400 MHz, MeOH-d_4): δ 3.92 (s, 3H), 4.44 (s, 2H), 6.53 (dd, $J = 7.5$, 5.4, 1H), 6.72 (dd, $J = 7.9$, 1.2, 1H), 7.33 (dd, $J = 5.1$, 1.4, 1H), 7.45 (d, $J = 5.1$, 1H), 7.51−7.56 (m, 2H), 7.66 (s, 1H), 8.20 (d, $J = 2.7$, 1H), 8.36 (d, $J = 1.8$, 1H). MS (+ES): *m*/*e* 307 (MH^+).

***N*³-[3-(5-Propoxypyridin-3-yl)benzyl]pyridine-2,3-diamine (6c)**. To a solution of 5-bromo-3-pyridinol (629 mg, 3.61 mmol) in DMF (10 mL) was added potassium carbonate (500 mg, 3.62 mmol), and the reaction stirred at room temperature. 1-Bromopropane (660 mg, 5.4 mmol) was then added and the reaction stirred for 18 h. The solvent was then removed *in vacuo*. The resulting material was partitioned between diethyl ether and H_2O, and the organics were washed with water, dried over $MgSO_4$, and evaporated to dryness. The material did not require further purification. The product was 3-bromo-5-propoxypyridine as a pale yellow liquid (660 mg, 85%). ^{1}H NMR (400 MHz, MeOH-d_4): δ 1.07 (t, $J = 7.4$, 3H), 1.79−1.88 (m, 2H), 4.04 (t, $J = 6.4$, 2H), 7.63 (t, $J = 2.2$, 1H), 8.22 (m, 2H). MS (+ES): *m*/*e* 216, 218 (MH^+). To 3-benzaldehydeboronic acid (300 mg, 2 mmol) were added 3-bromo-5-propoxypyridine (216 mg, 1 mmol) and potassium carbonate (828 mg, 6 mmol). Toluene (2 mL), ethanol (2 mL), and water (2 mL) were then added. Bis(tri-*tert*-butylphosphine)-palladium(0) (30 mg) was then added and the mixture vigorously stirred under nitrogen until all the reagents dissolved. The reaction was then heated to 130 °C for 30 min in a CEM microwave. The mixture was cooled to room temperature and then partitioned between DCM and H_2O, dried over $MgSO_4$, and evaporated to dryness. The crude material was purified by flash chromatography on silica to give 3-(5-propoxypyridin-3-yl)benzaldehyde (150 mg, 62%). ^{1}H NMR (400 MHz, $CDCl_3$): δ 1.02 (t, $J = 7.7$, 3H), 1.80 (sextet, $J = 7.2$, 2H), 4.00 (t, $J = 6.6$, 2H), 7.41 (m, 1H), 7.60 (t, $J = 8.0$, 1H), 7.76−7.80 (m, 1H), 7.86 (dt, $J = 7.6$, 1.2, 1H), 8.02 (d, $J = 2.2$, 1H), 8.26 (d, $J = 2.9$, 1H), 8.41 (d, $J = 1.6$, 1H), 10.03 (s, 1H). MS (+ES): *m*/*e* 242 (MH^+). 3-(5-Propoxypyridin-3-yl)benzaldehyde and 2,3-diaminopyridine were then treated under the conditions described above in the preparation of compound **6a** to give the title compound after purification by preparative HPLC/MS as its formic acid salt (38 mg, 37%). ^{1}H NMR (400 MHz, MeOH-d_4): δ 1.10 (t, $J = 7.4$, 3H), 1.87 (sextet, $J = 6.3$, 2H), 4.11 (t, $J = 6.4$, 2H), 4.53 (s, 2H), 6.73 (dd, $J = 7.9$, 5.9, 1H), 6.93 (d, $J = 7.8$, 1H), 7.27 (dd, $J = 1.3$, 5.8, 1H), 7.46−7.54 (m, 2H), 7.58−7.63 (m, 2H), 7.71 (s, 1H), 8.23 (d, $J = 2.8$, 1H), 8.28 (d, $J = 1.7$, 1H). MS (+ES): *m*/*e* 335 (MH^+).

***N*³-[3-(1*H*-Indol-6-yl)benzyl]pyridine-2,3-diamine (7)**. To a mixture of *N*³-(3-benzylboronic acid)pyridine-2,3-diamine **15b** (150 mg, 0.62 mmol) in DMF (3 mL) was added *tetrakis*(triphenylphosphine)palladium(0) (5 mg) followed by 6-bromoindole (120 mg, 0.62 mmol). Potassium phosphate (2 N, 1 mL) was then added, and the reaction was heated to 100 °C for 12 h. The mixture was cooled to room temperature and the solvent removed *in vacuo*. The resulting material was partitioned between DCM and H_2O, dried over $MgSO_4$, and evaporated to dryness. Material purified by preparative HPLC to give the title compound as a pale yellow solid. ^{1}H NMR (400 MHz, MeOH-d_4): δ 4.45 (s, 2H), 6.46 (d, $J = 3.3$, 1H), 6.58 (dd, $J = 7.8$, 5.3, 1H), 6.79 (d, $J = 9.0$, 1H), 7.27 (d, $J = 3.0$, 1H), 7.30−7.34 (m, 3H), 7.40 (t, $J = 7.5$, 1H), 7.56 (d, $J = 7.6$, 1H), 7.59−7.61 (m, 2H), 7.7 (s, 1H). MS (+ES): *m*/*e* 315 (MH^+).

2-Benzyloxy-5-bromobenzaldehyde (17a). Benzyl bromide (6.16 g, 36.0 mmol) was added to a stirred mixture of 5-bromo-2-hydroxybenzaldehyde **16** (6.03 g, 30.0 mmol) and anhydrous potassium carbonate (8.28 g, 60.0 mmol) in tetrahydrofuran (80 mL), and the mixture was stirred and held at reflux for 16 h. Upon cooling, the solvent was removed *in vacuo*, the mixture partitioned between dichloromethane and water, the organic layer separated, and the solvent removed *in vacuo*. The residue was triturated with 33% diethyl ether in petroleum ether, and the resulting solids were collected by suction filtration and sucked dry under reduced pressure to afford 7.65 g of **17a** as a colorless solid (88%). ^{1}H NMR (400 MHz, DMSO-d_6): δ 5.31 (s, 2H), 7.30−7.37 (m, 2H), 7.42 (t, $J = 7$, 2H), 7.51 (d, $J = 7$, 2H), 7.78 (d, $J = 2$, 1H), 7.83 (d, $J = 8$, 2, 1H), 10.34 (s, 1H). MS (+ES): *m*/*e* 292, 294 (MH^+).

Compound **17b** was prepared in a similar fashion to that outlined above for **17a**. For NMR and MS data of this compound, see Supporting Information.

***N*³-(2-Benzyloxy-5-bromobenzyl)pyridine-2,3-diamine (18a)**. A mixture of 2,3-diaminopyridine **14** (55 mg, 0.50 mmol), **17a** (192 mg, 0.50 mmol), and acetic acid (4 drops) in dichloromethane (3 mL) was stirred at room temperature for 10 min. Sodium triacetoxyborohydride (300 mg, 1.50 mmol) was added, and the mixture was stirred at room temperature overnight. The mixture was washed with an equal volume of 2 M sodium hydroxide solution, the organic layer separated, the solvent removed *in vacuo*, and the residue subjected to column chromatography on silica. Elution with 5% methanol in ethyl acetate afforded 82 mg of **18a** as a yellow oil (43%). ^{1}H NMR (400 MHz, DMSO-d_6): δ 4.29 (d, $J = 5.5$, 2H), 5.21 (s, 2H), 5.35 (t, $J = 5.5$, 1H), 5.52 (br s, 2H), 6.37 (d, $J = 3.5$, 2H), 7.08 (d, $J = 9$, 1H), 7.29 (t, $J = 3.5$, 1H), 7.33−7.42 (m, 5H), 7.50 (d, $J = 8.5$, 2H). MS (+ES): *m*/*e* 384, 386 (MH^+).

Compound **18b** was prepared in a similar fashion to that outlined above for **18a**. For NMR and MS data of this compound, see Supporting Information.

***N*³-[2-Benzyloxy-5-(1*H*-indol-6-yl)benzyl]pyridine-2,3-diamine (8a)**. A mixture of **18a** (77 mg, 0.2 mmol), indole-6-boronic acid (77 mg, 0.48 mmol), anhydrous potassium carbonate (166 mg, 1.20 mmol), and bis(tri-*tert*-butylphosphine)palladium(0) (4 mg) in methanol (0.7 mL), ethanol (0.7 mL), water (0.7 mL), and toluene (0.7 mL) was subjected to microwave irradiation (CEM microwave) at 135 °C for 15 min. The mixture was filtered, the organic solvent evaporated *in vacuo*, and the residue partitioned between dichloromethane and 2 M sodium hydroxide. The organic layer was separated, the solvent removed *in vacuo*, and the residue subjected to column chromatography on silica. Elution with 5% methanol in ethyl acetate afforded **8a** as a pale brown foam (40 mg, 48%).^{1}H

NMR (400 MHz, DMSO-d_6): δ 4.38 (d, J = 5.5, 2H), 5.26 (s, 2H), 5.35 (t, J = 5.5, 1H), 5.54 (br s, 2H), 6.37−6.41 (m, 2H), 6.52 (d, J = 7.5, 1H), 7.18 (d, J = 8.5, 2H), 7.27 (dd, J = 5, 1.5, 1H), 7.32−7.36 (m, 2H), 7.41 (t, J = 7, 2H), 7.50−7.59 (m, 6H), 11.10 (br s, 1H). MS (+ES): *m*/*e* 421 (MH^+).

Compound **8b** was prepared in a similar fashion to that outlined above for **8a**. For NMR and MS data of this compound, see Supporting Information.

Acknowledgment. The authors thank Harren Jhoti, Anne Cleasby, and Glyn Williams for their helpful advice and suggestions during the course of this research. We acknowledge the European Synchrotron Radiation Facility, Grenoble, and the Synchrotron Radiation Source, Daresbury, for access to beamtime.

Supporting Information Available: Additional spectral data for compounds **3**, **8b**, **11b**, **11c**, **12b**, **13a**, **15b**, **17b**, and **18b** and information on compound purity. This material is available free of charge via the Internet at http://pubs.acs.org.

References

(1) Hardy, J.; Selkoe, D. J. The amyloid hypothesis of Alzheimer's disease: progress and problems on the road to therapeutics. *Science* **2002**, *297*, 353−356.
(2) Sinha, S.; Lieberburg, I. Cellular mechanisms of beta-amyloid production and secretion. *Proc. Natl. Acad. Sci. U.S.A.* **1999**, *96*, 11049−11053.
(3) Hussain, I.; Powell, D.; Howlett, D. R.; Tew, D. G.; Meek, T. D.; Chapman, C.; Gloger, I. S.; Murphy, K. E.; Southan, C. D.; Ryan, D. M.; Smith, T. S.; Simmons, D. L.; Walsh, F. S.; Dingwall, C.; Christie, G. Identification of a novel aspartic protease (Asp 2) as beta-secretase. *Mol. Cell Neurosci.* **1999**, *14*, 419−427.
(4) Lin, X.; Koelsch, G.; Wu, S.; Downs, D.; Dashti, A.; Tang, J. Human aspartic protease memapsin 2 cleaves the beta-secretase site of beta-amyloid precursor protein. *Proc. Natl. Acad. Sci. U.S.A* **2000**, *97*, 1456−1460.
(5) Sinha, S.; Anderson, J. P.; Barbour, R.; Basi, G. S.; Caccavello, R.; Davis, D.; Doan, M.; Dovey, H. F.; Frigon, N.; Hong, J.; Jacobson-Croak, K.; Jewett, N.; Keim, P.; Knops, J.; Lieberburg, I.; Power, M.; Tan, H.; Tatsuno, G.; Tung, J.; Schenk, D.; Seubert, P.; Suomensaari, S. M.; Wang, S.; Walker, D.; Zhao, J.; McConlogue, L.; John, V. Purification and cloning of amyloid precursor protein beta-secretase from human brain. *Nature* **1999**, *402*, 537−540.
(6) Vassar, R.; Bennett, B. D.; Babu-Khan, S.; Kahn, S.; Mendiaz, E. A.; Denis, P.; Teplow, D. B.; Ross, S.; Amarante, P.; Loeloff, R.; Luo, Y.; Fisher, S.; Fuller, J.; Edenson, S.; Lile, J.; Jarosinski, M. A.; Biere, A. L.; Curran, E.; Burgess, T.; Louis, J. C.; Collins, F.; Treanor, J.; Rogers, G.; Citron, M. Beta-secretase cleavage of Alzheimer's amyloid precursor protein by the transmembrane aspartic protease BACE. *Science* **1999**, *286*, 735−741.
(7) Willem, M.; Garratt, A. N.; Novak, B.; Citron, M.; Kaufmann, S.; Rittger, A.; DeStrooper, B.; Saftig, P.; Birchmeier, C.; Haass, C. Control of peripheral nerve myelination by the beta-secretase BACE1. *Science* **2006**, *314*, 664−666.
(8) Cumming, J. N.; Iserloh, U.; Kennedy, M. E. Design and development of BACE-1 inhibitors. *Curr. Opin. Drug Discovery Dev.* **2004**, *7*, 536−556.
(9) John, V.; Beck, J. P.; Bienkowski, M. J.; Sinha, S.; Heinrikson, R. L. Human beta-secretase (BACE) and BACE inhibitors. *J. Med. Chem.* **2003**, *46*, 4625−4630.
(10) Chen, S. H.; Lamar, J.; Guo, D.; Kohn, T.; Yang, H. C.; McGee, J.; Timm, D.; Erickson, J.; Yip, Y.; May, P.; McCarthy, J. P3 cap modified Phe*-Ala series BACE inhibitors. *Bioorg. Med. Chem. Lett.* **2004**, *14*, 245−250.
(11) Lamar, J.; Hu, J.; Bueno, A. B.; Yang, H. C.; Guo, D.; Copp, J. D.; McGee, J.; Gitter, B.; Timm, D.; May, P.; McCarthy, J.; Chen, S. H. Phe*-Ala-based pentapeptide mimetics are BACE inhibitors: P2 and P3 SAR. *Bioorg. Med. Chem. Lett.* **2004**, *14*, 239−243.
(12) Hu, B.; Fan, K. Y.; Bridges, K.; Chopra, R.; Lovering, F.; Cole, D.; Zhou, P.; Ellingboe, J.; Jin, G.; Cowling, R.; Bard, J. Synthesis and SAR of bis-statine based peptides as BACE 1 inhibitors. *Bioorg. Med. Chem. Lett.* **2004**, *14*, 3457−3460.
(13) Ghosh, A. K.; Devasamudram, T.; Hong, L.; DeZutter, C.; Xu, X.; Weerasena, V.; Koelsch, G.; Bilcer, G.; Tang, J. Structure-based design of cycloamide-urethane-derived novel inhibitors of human brain memapsin 2 (beta-secretase). *Bioorg. Med. Chem. Lett.* **2005**, *15*, 15−20.
(14) Ghosh, A. K.; Bilcer, G.; Harwood, C.; Kawahama, R.; Shin, D.; Hussain, K. A.; Hong, L.; Loy, J. A.; Nguyen, C.; Koelsch, G.; Ermolieff, J.; Tang, J. Structure-based design: potent inhibitors of human brain memapsin 2 (beta-secretase). *J. Med. Chem.* **2001**, *44*, 2865−2868.
(15) Hom, R. K.; Gailunas, A. F.; Mamo, S.; Fang, L. Y.; Tung, J. S.; Walker, D. E.; Davis, D.; Thorsett, E. D.; Jewett, N. E.; Moon, J. B.; John, V. Design and synthesis of hydroxyethylene-based peptidomimetic inhibitors of human beta-secretase. *J. Med. Chem.* **2004**, *47*, 158−164.
(16) Hom, R. K.; Fang, L. Y.; Mamo, S.; Tung, J. S.; Guinn, A. C.; Walker, D. E.; Davis, D. L.; Gailunas, A. F.; Thorsett, E. D.; Sinha, S.; Knops, J. E.; Jewett, N. E.; Anderson, J. P.; John, V. Design and synthesis of statine-based cell-permeable peptidomimetic inhibitors of human beta-secretase. *J. Med. Chem.* **2003**, *46*, 1799−1802.
(17) Yang, W.; Lu, W.; Lu, Y.; Zhong, M.; Sun, J.; Thomas, A. E.; Wilkinson, J. M.; Fucini, R. V.; Lam, M.; Randal, M.; Shi, X. P.; Jacobs, J. W.; McDowell, R. S.; Gordon, E. M.; Ballinger, M. D. Aminoethylenes: a tetrahedral intermediate isostere yielding potent inhibitors of the aspartyl protease BACE-1. *J. Med. Chem.* **2006**, *49*, 839−842.
(18) Brady, S. F.; Singh, S.; Crouthamel, M. C.; Holloway, M. K.; Coburn, C. A.; Garsky, V. M.; Bogusky, M.; Pennington, M. W.; Vacca, J. P.; Hazuda, D.; Lai, M. T. Rational design and synthesis of selective BACE-1 inhibitors. *Bioorg. Med. Chem. Lett.* **2004**, *14*, 601−604.
(19) Hanessian, S.; Yun, H.; Hou, Y.; Yang, G.; Bayrakdarian, M.; Therrien, E.; Moitessier, N.; Roggo, S.; Veenstra, S.; Tintelnot-Blomley, M.; Rondeau, J. M.; Ostermeier, C.; Strauss, A.; Ramage, P.; Paganetti, P.; Neumann, U.; Betschart, C. Structure-based design, synthesis, and memapsin 2 (BACE) inhibitory activity of carbocyclic and heterocyclic peptidomimetics. *J. Med. Chem.* **2005**, *48*, 5175−5190.
(20) Clark, D. E. Rapid calculation of polar molecular surface area and its application to the prediction of transport phenomena. 2. Prediction of blood-brain barrier penetration. *J. Pharm. Sci.* **1999**, *88*, 815−821.
(21) Lipinski, C. A.; Lombardo, F.; Dominy, B. W.; Feeney, P. J. Experimental and computational approaches to estimate solubility and permeability in drug discovery and development settings. *Adv. Drug Delivery Rev.* **2001**, *46*, 3−26.
(22) Stachel, S. J.; Coburn, C. A.; Steele, T. G.; Jones, K. G.; Loutzenhiser, E. F.; Gregro, A. R.; Rajapakse, H. A.; Lai, M. T.; Crouthamel, M. C.; Xu, M.; Tugusheva, K.; Lineberger, J. E.; Pietrak, B. L.; Espeseth, A. S.; Shi, X. P.; Chen-Dodson, E.; Holloway, M. K.; Munshi, S.; Simon, A. J.; Kuo, L.; Vacca, J. P. Structure-based design of potent and selective cell-permeable inhibitors of human beta-secretase (BACE-1). *J. Med. Chem.* **2004**, *47*, 6447−6450.
(23) Coburn, C. A.; Stachel, S. J.; Li, Y. M.; Rush, D. M.; Steele, T. G.; Chen-Dodson, E.; Holloway, M. K.; Xu, M.; Huang, Q.; Lai, M. T.; DiMuzio, J.; Crouthamel, M. C.; Shi, X. P.; Sardana, V.; Chen, Z.; Munshi, S.; Kuo, L.; Makara, G. M.; Annis, D. A.; Tadikonda, P. K.; Nash, H. M.; Vacca, J. P.; Wang, T. Identification of a small molecule nonpeptide active site beta-secretase inhibitor that displays a nontraditional binding mode for aspartyl proteases. *J. Med. Chem.* **2004**, *47*, 6117−6119.
(24) Garino, C.; Pietrancosta, N.; Laras, Y.; Moret, V.; Rolland, A.; Quelever, G.; Kraus, J. L. BACE-1 inhibitory activities of new substituted phenyl-piperazine coupled to various heterocycles: chromene, coumarin and quinoline. *Bioorg. Med. Chem. Lett.* **2006**, *16*, 1995−1999.
(25) Huang, D.; Luthi, U.; Kolb, P.; Cecchini, M.; Barberis, A.; Caflisch, A. In silico discovery of beta-secretase inhibitors. *J. Am. Chem. Soc.* **2006**, *128*, 5436−5443.
(26) Huang, D.; Luthi, U.; Kolb, P.; Edler, K.; Cecchini, M.; Audetat, S.; Barberis, A.; Caflisch, A. Discovery of cell-permeable non-peptide inhibitors of beta-secretase by high-throughput docking and continuum electrostatics calculations. *J. Med. Chem.* **2005**, *48*, 5108−5111.
(27) Patel, S.; Vuillard, L.; Cleasby, A.; Murray, C. W.; Yon, J. Apo and inhibitor complex structures of BACE (beta-secretase). *J. Mol. Biol.* **2004**, *343*, 407−416.
(28) Hong, L.; Koelsch, G.; Lin, X.; Wu, S.; Terzyan, S.; Ghosh, A. K.; Zhang, X. C.; Tang, J. Structure of the protease domain of memapsin 2 (beta-secretase) complexed with inhibitor. *Science* **2000**, *290*, 150−153.
(29) Hong, L.; Turner, R. T., III; Koelsch, G.; Shin, D.; Ghosh, A. K.; Tang, J. Crystal structure of memapsin 2 (beta-secretase) in complex with an inhibitor OM00-3. *Biochemistry* **2002**, *41*, 10963−10967.
(30) The electron density for structure **2** indicated two binding modes where the phenyl substituent occupied either the S_2' and S_1 pockets.
(31) Although this compound reproducibly gave affinity in the 10 μM range (n = 6), the data always exhibited a high Hill slope. This data should therefore be treated with some caution. 2006.

(32) Guller, R.; Binggeli, A.; Breu, V.; Bur, D.; Fischli, W.; Hirth, G.; Jenny, C.; Kansy, M.; Montavon, F.; Muller, M.; Oefner, C.; Stadler, H.; Vieira, E.; Wilhelm, M.; Wostl, W.; Marki, H. P. Piperidine-renin inhibitors compounds with improved physicochemical properties. *Bioorg. Med. Chem. Lett.* **1999**, *9*, 1403−1408.
(33) Oefner, C.; Binggeli, A.; Breu, V.; Bur, D.; Clozel, J. P.; D'Arcy, A.; Dorn, A.; Fischli, W.; Gruninger, F.; Guller, R.; Hirth, G.; Marki, H.; Mathews, S.; ller, M.; Ridley, R. G.; Stadler, H.; Vieira, E.; Wilhelm, M.; Winkler, F.; Wostl, W. Renin inhibition by substituted piperidines: a novel paradigm for the inhibition of monomeric aspartic proteinases? *Chem. Biol.* **1999**, *6*, 127−131.
(34) Vieira, E.; Binggeli, A.; Breu, V.; Bur, D.; Fischli, W.; Guller, R.; Hirth, G.; Marki, H. P.; Muller, M.; Oefner, C.; Scalone, M.; Stadler, H.; Wilhelm, M.; Wostl, W. Substituted piperidines−highly potent renin inhibitors due to induced fit adaptation of the active site. *Bioorg. Med. Chem. Lett.* **1999**, *9*, 1397−1402.
(35) Hopkins, A. L.; Groom, C. R.; Alex, A. Ligand efficiency: a useful metric for lead selection. *Drug Discovery Today* **2004**, *9*, 430−431.
(36) After the submission of this paper, Cole et al. described the use of acylguanidines as inhibitors of BACE-1. These compounds exploit the same binding motif described in this work. Cole, D. C.; Manas, E. S.; Stock, J. R.; Condon, J. S.; Jennings, L. D.; Aulabaugh, A.; Chopra, R.; Cowling, R.; Ellingboe, J. W.; Fan, K. Y.; Harrison, B. L.; Hu, Y.; Jacobsen, S.; Jin, G.; Lin, L.; Lovering, F. E.; Malamas, M. S.; Stahl, M. L.; Strand, J.; Sukhdeo, M. N.; Svenson, K.; Turner, M. J.; Wagner, E.; Wu, J.; Zhou, P.; Bard, J. Acylguanidines as small-molecule beta-secretase inhibitors. *J. Med. Chem* **2006**, *49*, 6158−6161. There have also been two recent patent applications containing aminopyridines and their potential use as BACE-1 inhibitors. (a) Coburn, C. A.; Holloway, M. K.; Stachel, S. J. 2-aminopyridines compounds useful as beta-secretase inhibitors for the treatment of Alzheimer's disease. PCT Int. Appl. WO 2006060109, **2006**. (b) Albert, J. S.; Callaghan, O.; Campbell, J.; Carr, R. A. E.; Chessari, G.; Cowan, S.; Congreve, M.S.; Edwards, P.; Frederickson, M.; Murray, C. W.; Patel, S. Substituted aminopyridines and uses thereof. PCT Int. Appl. WO2006065204, 2006.
(37) Leslie, A. G. W.; Brick, P.; Wonacott, A. MOSFLM. *Daresbury Lab. Inf. Quart. Protein Crystallogr.* **2004**, *18*, 33−39.
(38) Collaborative Computational Project, N. 4. The CCP4 suite: programs for protein crystallography. *Acta Crystallogr*. **1994**, *D50*, 760−763.
(39) Mooij, W. T.; Hartshorn, M. J.; Tickle, I. J.; Sharff, A. J.; Verdonk, M. L.; Jhoti, H. Automated protein-ligand crystallography for structure-based drug design. *ChemMedChem.* **2006**, *1*, 827−838.
(40) Hartshorn, M. J. AstexViewer: a visualisation aid for structure-based drug design. *J. Comput.-Aided Mol. Des.* **2002**, *16*, 871−881.
(41) Winn, M. D.; Isupov, M. N.; Murshudov, G. N. Use of TLS parameters to model anisotropic displacements in macromolecular refinement. *Acta Crystallogr. D: Biol. Crystallogr.* **2001**, *57*, 122−133.
(42) Watson, P.; Verdonk, M. L.; Hartshorn, M. J. A web-based platform for virtual screening. *J. Mol. Graph. Model.* **2003**, *22*, 71−82.
(43) Verdonk, M. L.; Cole, J. C.; Hartshorn, M.; Murray, C. W.; Taylor, R. D. Improved protein-ligand docking using GOLD. *Proteins* **2003**, *52*, 609−623.
(44) Khanna, I. K.; Weier, R. M.; Lentz, K. T.; Swenton, L.; Lankin, D. C. Facile, regioselective syntheses of N-alkylated 2,3-diaminopyridines and imidazo[4,5-*b*]pyridines. *J. Org. Chem* **1995**, *60*, 960−965.

JM061197U